

Research Article

Competitive Adsorption of Anionic Dyes from Aqueous Single and Binary Solutions with CoAl Layered Double Hydroxide

Ime Akanyeti^{1,2,*} , Jamilu Abdullahi^{2,3} 

¹ Cyprus International University, Faculty of Engineering, Department of Environmental Engineering, Haspolat, Lefkoşa, North Cyprus, Mersin 10, TURKIYE

² Cyprus International University, Environmental Research Centre, Haspolat, Lefkoşa, North Cyprus, Mersin 10, TURKIYE

³ Cyprus International University, Institute of Graduate Studies and Research, Environmental Engineering, Haspolat, Lefkoşa, North Cyprus via Mersin 10, TURKIYE

* Corresponding author: I. Akanyeti
E-mail: iakanyeti@ciu.edu.tr

Received:26.08.2022

Accepted 02.09.2023

How to cite: Akanyeti and Abdullahi, (2023). Competitive Adsorption of Anionic Dyes from Aqueous Single and Binary Solutions with CoAl Layered Double Hydroxide. *International Journal of Environment and Geoinformatics (IJECEO)*, 10(3): 065-076, doi. 10.30897/ijegeo.1167267

Abstract

Layered double hydroxides (LDH) have been extensively studied as high-capacity adsorbents for dye removal from water. However, a comprehensive understanding of why one dye is adsorbed more than another remains unknown. In addition, very little is known about how the adsorption mechanisms scale when more than one dye is present in the solution. The adsorption capacity of cobalt-aluminum (CoAl) LDH was investigated for methyl orange (MO), remazol brilliant blue (RBBR), and allura red (AR) at different dye concentrations. The maximum mass of dye adsorbed was obtained for MO (2.267 mmol/g), followed by RBBR (0.258 mmol/g) and AR (0.195 mmol/g). X-ray diffraction and Fourier transform infrared analysis results demonstrated that surface adsorption and electrostatic interactions contributed to adsorption, while intercalation did not. In a binary solution of MO and RBBR, the highest mass of adsorbed MO was reduced to 1.521 mmol/g, whereas the maximum RBBR mass adsorbed increased to 0.268 mmol/g. CoAl LDH preferentially adsorbed RBBR within a concentration range of up to 0.026 mmol/L, while MO was preferred at higher concentrations. Overall, the findings suggest that the adsorption capacity of an LDH is highly dependent on the number, characteristics, and equilibrium concentrations of the dyes present in the solution.

Keywords: Layered double hydroxide, Adsorption, Methyl orange, Remazol brilliant blue, Binary solution

Introduction

Synthetic dyes released by effluents from various industries have been detected in water bodies and cause environmental pollution (Slama et al., 2021). There are many adverse impacts of persistent dyes in aquatic environments such as inhibition of photochemical activities (Pereira and Alves, 2012) and carcinogenic effects on living organisms (Chung, et al., 1981; Golka, et al., 2004)

Conventional wastewater treatments are not efficient enough to remove these synthetic dyes because of their persistent characteristics, such as non-biodegradability and chemical stability (Wong and Yu, 1999). To date, many methods, including adsorption, chemical oxidation, photodegradation and microbial decoloration / degradation, have been widely used for dye removal (Forgacs, et al., 2004). Adsorption is considered an economical and technically viable process with good performance for removing synthetic dyes from water at low operating costs (Geethakarathi, A. and Phanikumar, 2011; Kumar et al., 2019).

Layered double hydroxides (LDH) have recently received attention as high-capacity adsorbents for water pollutants owing to their large surface area, high anion exchange

capacity, water resistance, and high thermal stability (Sajid and Basheer, 2016). The synthesis of LDH is economical because of the common and abundant metals in their structures. Faster kinetics and full regeneration capacities in a short time for reuse are advantages of LDH compared to other adsorbents (Goh, et al., 2008).

The adsorption of dyes on LDH made of different metal hydroxide combinations and prepared using various methods has been studied extensively (Abdellaoui, et al., 2017; Aguiar et al., 2013; de Sá, Cunha, and Nunes, 2013; Gidado and Akanyeti, 2020; Guo, et al., 2013; Ni, et al., 2007). However, understanding why one dye is adsorbed more than another requires clarification (Goh et al., 2008; Yagub et al., 2014). Studies on competitive dye adsorption on various adsorbents have shown that adsorption capacity is influenced by the presence of different dyes in the solution (Chiou and Chuang, 2006; Turabik and Gozmen, 2013; Zhu et al., 2020). Nevertheless, further investigation is required to fully understand how the adsorption affinity of LDH changes when more than one dye is present in the solution.

MO is a reactive azo dye used in various industries including textiles and cosmetics. The adsorption of MO on LDH has been studied extensively by many researchers as a model dye (Ni et al. 2007; Monash and Pugazhenthir 2014; Lu et al. 2016; Ling et al. 2016; Hassani et al. 2017).

Remazol brilliant blue reactive (RBBR) is a toxic and refractory organopollutant and commonly used in the textile and dye production industries (Ada, et al., 2009). Allura red (AR) is another azo dye that is widely used in the food and cosmetic industries, with a debate on its potential security risks (Esmaeili et al., 2016). Studies on the adsorption of RBBR (Elkhatabi et al., 2013; Gidado and Akanyeti, 2020) and AR (Choy et al., 2008; Sohrabi et al., 2023) on LDH powder are limited. Various dyes can be present simultaneously in water resources as pollutants to be treated owing to industrial discharge.

In this study, CoAl LDH was prepared using a simple co-precipitation method and used as an adsorbent to remove MO, RBBR, and AR from aqueous single and binary solutions. The adsorption affinity and mechanisms of CoAl LDH for RBBR were studied for the first time in comparison to those of two azo dyes, MO and AR, in

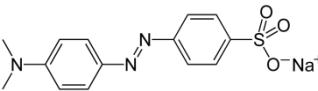
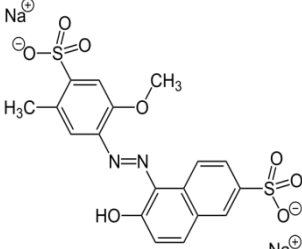
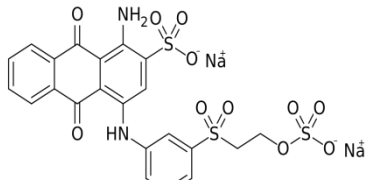
single dye solutions. Moreover, the adsorption capacity of CoAl LDH in a binary dye solution of RBBR and MO was elucidated, shedding more light on the competitive adsorption affinity.

Materials and Methods

Chemicals

Analytical grade $\text{Co}(\text{NO}_3)_2 \cdot 6\text{H}_2\text{O}$ ($\geq 99\%$), $\text{Al}(\text{NO}_3)_3 \cdot 9\text{H}_2\text{O}$ ($\geq 95\%$), MO ($\geq 95.0\%$) and ammonia ($\text{NH}_3 \cdot \text{H}_2\text{O}$, 28-30%) were purchased from Merck (Darmstadt, Germany). AR (80%) and RBBR (50%) were purchased from Sigma-Aldrich (USA). The characteristics of the dyes are presented in Table 1. Distilled water produced using Sartorius 61316 and 611 UV ultrapure water system (UK) was used to prepare the experimental solutions.

Table 1 Physical and chemical characteristics of dyes

Name	Molecular Formula & (Molecular Weight, g/mol)	Chemical Structure	Molecular Size* (nm)	Molecular Width & Length & Height (Å°)	pK _a
Methyl Orange (MO)	$\text{C}_{14}\text{H}_{14}\text{N}_3\text{NaO}_3\text{S}$ (327.3)		1.315 ^a	5.5 & 15 ^b	3.46 ^c
Allura Red (AR)	$\text{C}_{18}\text{H}_{14}\text{N}_2\text{Na}_2\text{O}_8\text{S}_2$ (496.4)		~1 ^d	NA	<0.3 ^e
Remazol Brilliant Blue Reactive (RBBR)	$\text{C}_{22}\text{H}_{16}\text{N}_2\text{Na}_2\text{O}_{11}\text{S}_3$ (626.5)			13 & 26 & 8.5 ^f 11.3 & 18.4 ^g	<1 ^h

^athe length of the long side (Ni et al., 2007), ^b(Huang et al., 2017), ^c(Zaghouane et al., 2012b), ^dapproximated diameter et al., 2014) ^e(Bevziuk et al., 2017) ^f(Yahya, et al., 2016), ^g(Silva et al., 2016), ^h (Momenzadeh, et al., 2011; Saquib and Muneer, 2002)

Preparation and characterization of CoAl LDH

CoAl LDH with a 4:1 molar ratio of $\text{Co}^{2+}/\text{Al}^{3+}$ was prepared by the co-precipitation method as described by Ling et al., (2016). Briefly, 5.80 g of $\text{Co}(\text{NO}_3)_2 \cdot 6\text{H}_2\text{O}$ was mixed with 1.88 g of $\text{Al}(\text{NO}_3)_3 \cdot 9\text{H}_2\text{O}$ in 25 mL distilled water, making a total cation concentration of 1 M. 20 mL of the solution was then added drop wise at 2 mL/min into 100 mL of a 0.5 M ammonia solution under constant mixing and then stirred for 30 minutes. The suspension formed was aged at 65°C for 18 hours under constant mixing and then centrifuged for 30 minutes at 3824xG, (6000 rpm). The pellet was repeatedly washed with distilled water to remove the trace of unreacted nitrates and then oven dried at 65°C for 24 hours.

The crystallinity of LDH was characterized with an Ultima IV powder X-ray diffractometer (XRD) (Rigaku) at 40 kV, 20 mA, $\text{CuK}\alpha$ radiation (λ : 0.154056 nm), in the reflection scanning mode from $2\theta=10$ to 80° at a scan rate of $1^\circ/\text{min}$. Fourier transform infrared (FT-IR) spectra were recorded in the wavelength range of 400-4000 cm^{-1} using an IR Prestige-21 FT-IR Spectrophotometer (Shimadzu, Japan). FT-IR and XRD analysis were conducted before and after the adsorption of each dye on CoAl LDH. The zero point charge (pH_{zpc}) of LDH was determined using a titration method adapted from Wang and Reardon (2001). The sorbent (0.1 g) was added to 9 mL of distilled water. The solution pH was adjusted, and readings were recorded after 15 min. A KCl solution (0.005 M) was prepared by adding 0.5 mL of 0.1 M KCl in each solution and bringing

the volume to 10 mL using distilled water. The 0.005 M solutions were mixed for one hour in a shaker at 25°C and 200 rpm, and the pH (pH0.005M) in each bottle was recorded. 0.5 mL of 2 M KCl was added to each bottle, bringing the KCl molarity up to 0.1 M, and the pH (pH0.1M) was recorded for the last time while swirling the solution. For each sample, the difference between pH0.1M and pH0.005M was calculated and plotted against pH0.005M to determine the zero-point charge.

Adsorption Experiments

Dye solutions of 0.008-0.580 mmol/g for MO, RBBR, and AR were prepared using the stock dye solutions. For each experiment, 26 mg of LDH was added to a flask containing 130 mL of dye solution, except for the blank experiments, where no LDH was added. The solutions were mixed throughout the experiment at 150 rpm at 25±1°C in a water bath. The solution pH was not adjusted but was measured throughout the experiments. For all experiments, the solution pH was around pH 7.0±0.2. The initial sample was taken before the LDH was added to the solution. After the LDH was added, at various time intervals, 4 mL of samples were collected and centrifuged for 15 minutes at 3824xG (6000 rpm) at 25°C. The absorbance of the dye in the supernatant was measured using a UV-2450 UV-visible spectrophotometer (Shimadzu, Japan) at maximum light absorption wavelengths (λ_{max}) of 463 nm, 593 nm, and 498 nm for MO, RBBR, and AR, respectively. The calibration curve with $R^2 > 0.99$ for all three dyes in single and binary solutions was obtained for a concentration range of 0-35 mg/L. Solutions with dye concentrations above the calibration curve range were diluted before the analysis. Binary solutions of MO and RBBR, each dye at a concentration range of 0.008-0.580 mmol/g were prepared from a binary stock solution. The same experimental conditions were used for both the single- and binary-solution experiments.

Data Analysis

The amount of dye adsorbed onto LDH, Q_t (mmol/g) at time t (min) was determined using equation 1, where V is the volume of the dye solution (L), C_0 (mmol/L) is the initial dye concentration, C_t (mmol/L) is the concentration of the dye in the solution at time t and m (mg) is the mass of the LDH used.

$$Q_t = \frac{(C_0 - C_t)V}{m} \quad (\text{Eq.1})$$

For adsorption isotherms, the amount of dye adsorbed on LDH at equilibrium Q_e (mmol/g), was calculated using equation 2, where C_e (mmol/L) is the equilibrium dye concentration.

$$Q_e = \frac{(C_0 - C_e)V}{m} \quad (\text{Eq.2})$$

For the adsorption kinetics, the non-linear form of the pseudo-first and second-order reaction model equations are given in equations 3 and 4, respectively, where k_1 (1/min) and k_2 (g/mmol.min) are the rate constants.

$$Q_t = Q_e(1 - e^{-k_1 t}) \quad (\text{Eq.3})$$

$$Q_t = \frac{Q_e^2 k_2 t}{1 + k_2 Q_e t} \quad (\text{Eq.4})$$

The Elovich chemisorption model is presented in equation 5, where α (mmol/g.min) is the initial adsorption rate and β (g/mmol) is related to the extent of surface coverage and the activation energy involved in chemisorption.

$$Q_t = \frac{1}{\beta} \ln(1 + \alpha \beta t) \quad (\text{Eq.5})$$

Freundlich, Langmuir, Redlich-Peterson, Dubinin-Radushkevich and Brunauer-Emmett-Teller (BET) isotherm models were used to describe the adsorption of the dyes on CoAl LDH. The non-linear form of the Freundlich and Langmuir isotherm models, are given in equations 6 and 7, respectively, where k_F and n are the Freundlich constants indicating the dye adsorption capacity and intensity, Q_m (mmol/g) is the maximum dye adsorption capacity of LDH, and k_L (L/mmol) is the Langmuir constant.

$$Q_e = k_F C^n \quad (\text{Eq.6})$$

$$Q_e = \frac{Q_m k_L C_e}{1 + k_L C_e} \quad (\text{Eq.7})$$

The non-linear equation of Redlich-Peterson and Dubinin-Radushkevich isotherms are provided in equations 8 and 9, respectively where K_{RP} (L/g), a_{RP} (mmol/L)^{-g} are the Redlich-Peterson constants and g is the dimensionless exponent the value of which should be $0 < g \leq 1$, Q_{DR} (mmol/g) is the adsorption capacity, K_{DR} (mol²/kJ²) is a constant related to the adsorption energy, E (kJ/mol) is the mean adsorption energy which can be obtained by $\frac{1}{\sqrt{2K_{DR}}}$ and ϵ is the Polanyi potential.

$$Q_e = \frac{K_{RP} C_e}{1 + a_{RP} C_e^g} \quad (\text{Eq.8})$$

$$Q_e = Q_{DR} e^{-K_{DR} \epsilon^2} \quad (\text{Eq.9})$$

The non-linear equation of the BET model is given in equation 10, where K_S (L/mmol) is the equilibrium constant of adsorption for first layer in BET isotherms and K_L (L/mmol) is the equilibrium constant of adsorption for upper layers in BET isotherm.

$$Q_e = Q_m \frac{K_S C_e}{(1 - K_L C_e)(1 - K_L C_e + K_S C_e)} \quad (\text{Eq.10})$$

Randomly selected experiments were repeated at least twice and the reliability of the data was confirmed.

Results and Discussion

Adsorption kinetics of MO, RBBR and AR in single dye solutions

The results presented in Figure 1a-b show that MO adsorption on CoAl was the fastest among the three dyes, reaching equilibrium in 70 min for initial MO concentrations of 0.015, 0.031, and 0.061 mmol/L, and 450 min for initial MO concentrations of 0.153 and 0.306 mmol/L. For RBBR (Figure 1c-d), at 450 min, equilibrium was reached for the initial dye concentration of 0.016 mmol/L, 1400 min for 0.032 mmol/L, and 1600 min for 0.080, 0.160, and 0.319 mmol/L, respectively. For

AR, the system reached equilibrium in 200 min for 0.010 mmol/L, 1400 min for 0.020, 0.040, and 0.101 mmol/L, and 1600 min for 0.201 mmol/L initial AR concentrations (Figure 1e-f). In order to explain the kinetics of the dye adsorption on CoAl LDH, pseudo-first-order (equation 3), pseudo-second-order (equation 4) and Elovich models (equation 5) were fit to the data for each dye separately as shown in Figure 1. The adjusted coefficient of determination (R_{adj}^2) and root of mean square error (SD) obtained for each dye at various initial dye concentrations are presented in Table 2. The R_{adj}^2 (>0.99) values showed that a pseudo-second-order model described the adsorption kinetics for MO better than the other models. At all initial MO concentrations, the experimental dye adsorption capacity $Q_{e(exp)}$, agrees well with the theoretical capacity, $Q_{e(the)}$, calculated using the second-order model equation. For MO, the pseudo-second-order rate constant, k_2 , decreased from 6.715 to 0.170

g/(min.mmol) as the initial dye concentration increased from 0.015 to 0.306 mmol/L, indicating that the adsorption slowed down as the initial dye concentration increased (Table 2).

For RBBR and AR, the highest R_{adj}^2 (>0.97) values were obtained with Elovich equation, supporting a chemisorption nature (McIntok, 1967) of both dyes on CoAl LDH. Elovich equation is often valid for adsorption systems including sorbents with heterogeneous surface and the equation covers a wide range of slow adsorption rates (Lima, et al., 2015). The constant β , related to the extent of surface coverage, decreased from 140 to 31 g/mmol when the initial RBBR concentration increased from 0.016 to 0.319 mmol/L. Similarly, for AR, β decreased from 172 to 44 g/mmol when the initial dye concentration was increased from 0.010 to 0.201 mmol/L.

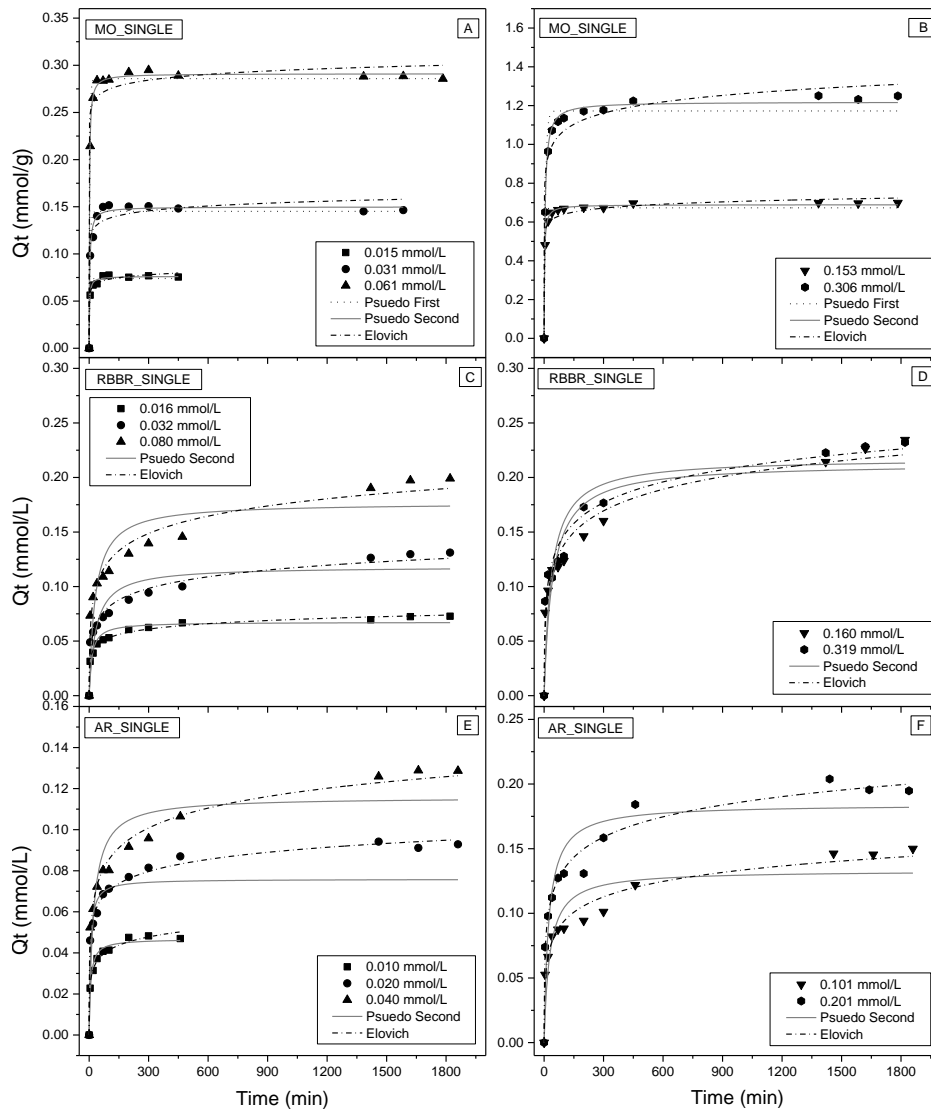


Fig. 1 Time dependent dye adsorption of a) MO (C_0 :0.015-0.061 mmol/L), b) MO (C_0 :0.153-0.306 mmol/L), c) RBBR (C_0 :0.016-0.080 mmol/L), d) RBBR (C_0 :0.160-0.319 mmol/L), e) AR (C_0 :0.010-0.040 mmol/L) and f) AR (C_0 :0.101-0.201 mmol/L) on CoAl LDH.

Table 2 Coefficients of adsorption kinetic models for MO, RBBR and AR in single dye solutions.

SINGLE		First order					Second order					Elovich	
C ₀ mmol/L	Q _{e(exp)} mmol/g	R ₂	SD	k ₁ 1/min	Q _{e(the)} mmol/g	R ₂	SD	k ₂ g/min.mmol	Q _{e(the)} mmol/g	R ₂	SD	α mmol/g.min	β g/mmol
MO													
0.015	0.076	0.97	0.004	0.281	0.074	0.99	0.002	6.715	0.076	0.98	0.003	226.9	708.6
0.031	0.146	0.95	0.009	0.208	0.145	0.98	0.006	2.247	0.150	0.93	0.012	1154.7	137.0
0.061	0.286	0.99	0.007	0.273	0.286	1.00	0.003	1.934	0.291	0.97	0.015	3.2x10 ⁹	113.7
0.153	0.699	0.98	0.027	0.244	0.673	1.00	0.010	0.632	0.689	0.97	0.032	1.0x10 ⁶	34.35
0.306	1.250	0.96	0.074	0.135	1.172	0.99	0.026	0.170	1.219	0.95	0.077	325.0	12.03
RBBR													
0.016	0.073	0.82	0.009	0.046	0.064	0.92	0.006	1.140	0.067	0.99	0.002	0.124	140.3
0.032	0.131	0.70	0.021	0.020	0.110	0.83	0.016	0.256	0.118	0.98	0.006	0.031	65.31
0.080	0.203	0.67	0.033	0.023	0.164	0.80	0.026	0.188	0.177	0.97	0.010	0.023	40.73
0.160	0.234	0.71	0.038	0.015	0.198	0.83	0.029	0.110	0.213	0.97	0.012	0.036	35.01
0.319	0.232	0.72	0.037	0.016	0.206	0.84	0.029	0.126	0.217	0.97	0.013	0.030	31.02
AR													
0.010	0.054	0.76	0.005	0.354	0.143	0.97	0.003	2.891	0.047	0.99	0.002	0.072	172.1
0.020	0.093	0.82	0.010	0.149	0.071	0.92	0.007	2.078	0.076	0.99	0.002	0.336	117.8
0.040	0.135	0.72	0.020	0.030	0.108	0.84	0.015	0.404	0.116	0.99	0.004	0.064	71.76
0.101	0.173	0.70	0.024	0.026	0.123	0.83	0.018	0.270	0.133	0.97	0.007	0.040	58.13
0.201	0.195	0.75	0.029	0.029	0.172	0.87	0.022	0.236	0.184	0.98	0.009	0.086	44.30

Adsorption in single dye solutions

Figure 2 presents the dye molar mass adsorbed on CoAl-LDH versus the equilibrium dye concentration for MO, AR and RBBR in single dye solutions.

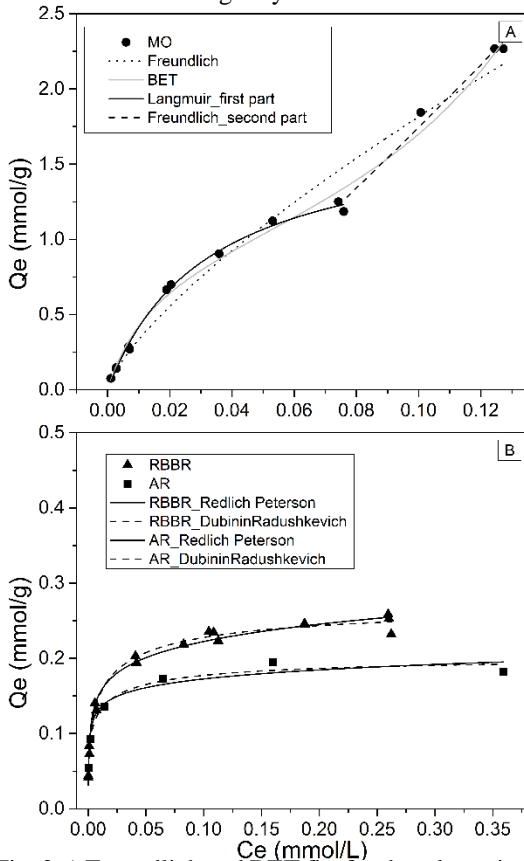


Fig. 2 a) Freundlich and BET fits for the adsorption of MO (C_e range: 0.00-0.13 mmol/L), Langmuir fit for the adsorption of MO (C_e range: 0.00-0.08 mmol/L), Freundlich fit for the adsorption of MO (C_e range: 0.08-0.13 mmol/L) b) Redlich Peterson and Dubinin Radushkevich fits for the adsorption data of RBBR and AR on CoAl-LDH in single dye solutions.

The largest amount of MO adsorbed on CoAl-LDH (2.267 mmol/g) was much higher than that adsorbed on RBBR and AR. In contrast, the maximum RBBR mass adsorbed (0.258 mmol/g) was larger than that for AR (0.195 mmol/g). To further explain the adsorption affinity of CoAl-LDH for the three dyes, various dye characteristics

and the potential for intermolecular interactions were considered.

All three dyes were negatively charged in the experimental solution (pH 7.0±0.2), considering the dissociation constants (pK_a) given in Table 1. The zero-point charge of CoAl LDH was obtained at a solution pH of 8, as displayed in Figure 3.

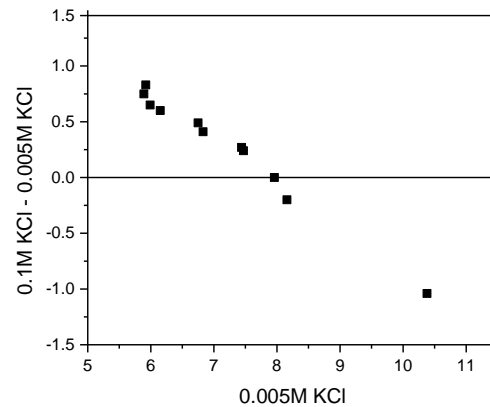


Fig. 3 The zero point charge of CoAl LDH. Therefore, the electrostatic interactions between the negatively charged dye molecules and the positively charged CoAl LDH are expected to contribute to adsorption.

In Figure 4, the diffraction patterns of Co-Al LDH before and after the adsorption of the dyes are presented. The well prepared crystalline structure of Co-Al LDH was demonstrated by the diffraction peaks obtained at 11.27°, 22.63°, 34.07°, 45.70° and 59.99° with interlayer space of 0.78, 0.39, 0.26, 0.20 and 0.15 nm, respectively, agreeing well with the pattern reported by Zubair et al., (2017). The intensities of the XRD peaks, especially those of (003) and (006), were reduced. The intensity reduction was correlated with the adsorbed dye mass. For example, the intensity reduction of MO was higher than those of RBBR and AR.

The basal spacing of the intrinsic CoAl LDH is d₀₀₃=0.78 nm and the layer thickness of brucite like materials is 0.48 nm (Darmograi et al., 2015). Subtracting the layer thickness of the brucite-like layer (0.48 nm) from the basal spacing, the interlayer space is calculated as 0.30

nm, similar to the diameter of a nitrate ion (0.40 nm) (Ay et al., 2009; Darmograi et al., 2015) present in between the double layers. The basal spacing of the CoAl LDH after dye adsorption was calculated as 0.79 nm, 0.79 nm and 0.78 nm for MO, RBBR and AR, respectively. Unlike other studies (Elkhattabi et al., 2013; Ling et al., 2016), in this study, no change was observed in the basal spacing after dye adsorption. Therefore, external surface adsorption is expected to play a role in the adsorption of the three dyes on the CoAl LDH. The dye molecules are three-dimensional, and it is possible that the smallest dimension of the MO was aligned with the interlayer spacing without causing any substantial change in the basal spacing.

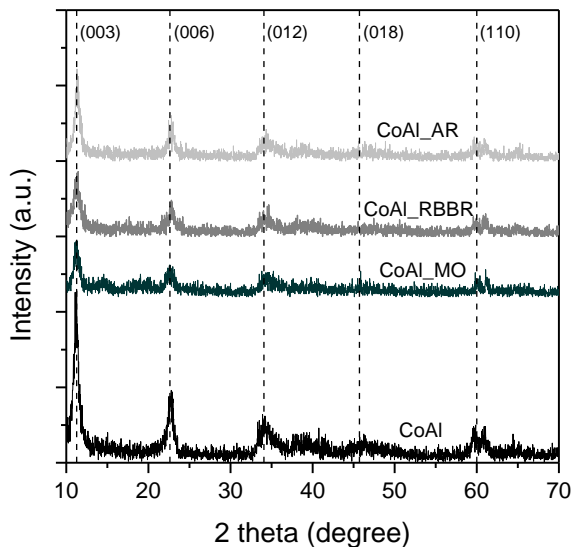


Fig. 4 X-ray patterns of CoAl LDH samples before and after the adsorption of MO, RBBR and AR.

In Figure 5, the FT-IR spectra of each dye together with the scan of Co-Al LDH before and after dye adsorption are displayed for MO(a), RBBR(b), and AR(c), respectively. The FT-IR peaks obtained for the Co-Al LDH before adsorption are in agreement with those reported by Zubair et al. (2017). The peak at 1634 cm^{-1} was attributed to the O-H bending vibration of water molecules, and the peak near 1350 cm^{-1} corresponded to the bending vibrations of N-O (the nitrate ions in between the layers). In Figure 5a, the spectrum of MO displays a peak near 1600 cm^{-1} for the C=C-C aromatic ring stretch, near 1365 cm^{-1} and 1190 cm^{-1} for the C-N vibrations, and near 1110 cm^{-1} for the S=O vibration. In Figure 5b, the spectrum of RBBR presents a peak near 1500 cm^{-1} and 1600 cm^{-1} for the C=C-C aromatic ring stretch and near 1200 cm^{-1} and 1100 cm^{-1} for the S=O vibration. In Figure 5c, the spectrum of AR displays a peak near 1065 cm^{-1} and 1180 cm^{-1} for the S=O vibration and near 1400 cm^{-1} , 1500 cm^{-1} , and 1620 cm^{-1} for the skeletal vibration of the benzene ring.

Comparing Figure 5a, b, and c, it was observed that the peak for the nitrate ion near 1350 cm^{-1} disappeared for CoAl LDH after adsorption of MO. However, the spectra of CoAl after the adsorption of RBBR and AR showed that the nitrate peak was still present, but at a lower intensity. As demonstrated by the XRD data in Figure 4,

intercalation did not occur, and dye molecules were mainly adsorbed on the surface. Adsorption possibly occurred by ligand exchange, where OH^- or H_2O groups on the surface were displaced by dye molecules (Gidado and Akanyeti, 2020; Lei, et al., 2014). The positive charge of the LDHs was possibly balanced by the negatively charged dye molecules adsorbed; hence, fewer nitrate anions were intercalated than those present in the CoAl LDH before adsorption. A larger amount of adsorbed MO possibly resulted in the release of almost all the nitrate ions, resulting in the disappearance of the nitrate peak.

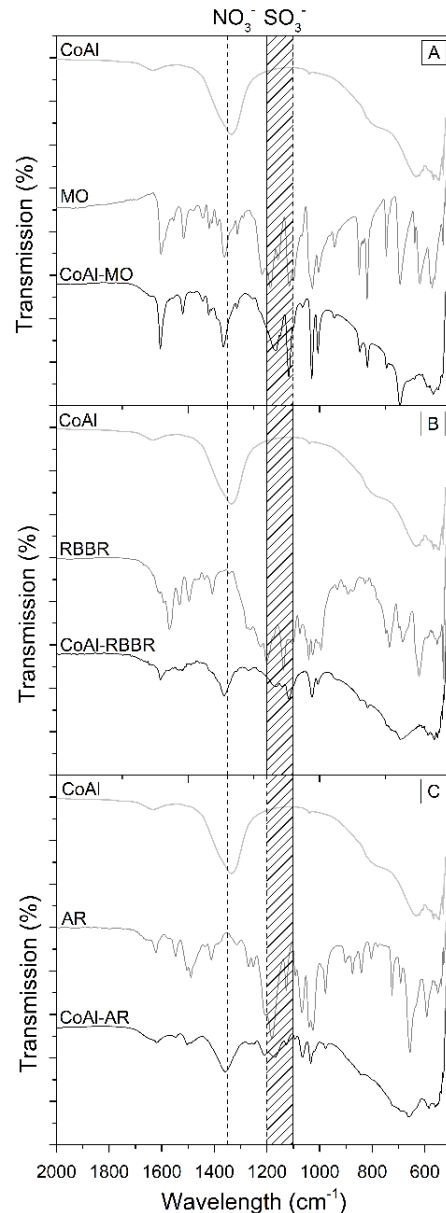


Fig. 5. FT-IR scan of the dye, CoAl LDH before and after the adsorption for MO (a), RBBR (b) and AR (c), ---- FT-IR peak for NO_3^- ions in between the LDH, // FT-IR peak interval for sulfonic group (SO_3^-) on dye molecule

However, the nitrate peaks were still present when RBBR and AR were adsorbed in smaller quantities. The presence of the S=O vibration on CoAl LDH after the adsorption of all dyes indicated that the dye molecules were adsorbed on LDH. The much higher S=O peak intensities for MO

compared to those of RBBR and AR is further evidence of the high affinity of CoAl LDH for MO.

The molecular structures of the dyes in Table 1 show that MO contains two hydrophobic methyl groups, besides SO_3^- , while RBBR contains hydrophilic C=O and NH_2 groups (Table 1). AR contains a hydrophobic methyl group and hydrophilic OH group, which reduces the hydrophobicity of the molecule. The hydrophobic characteristics of MO in comparison to the hydrophilic AR and RBBR molecules may also explain why a larger amount of MO was adsorbed on the LDH. Unlike RBBR and AR, once the MO molecules are adsorbed on LDH, the hydrophilic character of LDH is likely to become hydrophobic. Hence, hydrophobic interactions might contribute to enhancing the adsorption capacity of LDH

Table 3 Isotherm parameters for dye adsorption on CoAl-LDH in single and binary dye solutions.

Isotherm	Parameter	Unit	Single			Binary	
			MO	RBBR	AR	MO	RBBR
Langmuir	R_{adj}^2		0.959	0.933	0.870	0.952	0.989
	SD	mmol/g	0.155	0.020	0.020	0.108	0.011
	Q_m	mmol/g	6.407	0.238	0.178	10.88	0.280
	K_L	L/mmol	4.026	281.9	592.3	0.508	283.6
Freundlich	R_{adj}^2		0.974	0.958	0.890	0.962	0.828
	SD	mmol/g	0.124	0.016	0.018	0.097	0.043
	K_F	mmol/g. (mmol/L) ^{-1/n}	9.875	0.345	0.237	3.718	0.418
	n		0.736	0.201	0.150	0.809	0.218
Redlich-Peterson	R_{adj}^2		-	0.984	0.940	-	0.986
	SD	mmol/g	-	0.010	0.013	-	0.012
	K_{rp}	L/g	-	242.0	277.0	-	80.40
	A_{rp}	(mmol/L) ^g	-	789.0	1290	-	284.5
Dubinin-Radushkevich	R_{adj}^2		-	0.990	0.980	-	0.936
	SD	mmol/g	-	0.008	0.008	-	0.026
	Q_{dr}	mmol/g	-	0.265	0.199	-	0.320
	K_{dr}	mol ² /kJ ²	-	0.004	0.003	-	0.005
	E	kJ/mol	-	11.18	12.91	-	10.14
BET	R_{adj}^2		0.991	-	-	0.984	-
	SD	mmol/g	0.073	-	-	0.063	-
	K_L	L/mmol	4.728	-	-	2.253	-
	K_S	L/mmol	68.37	-	-	40.59	-
	Q_m	mmol/g	0.965	-	-	0.507	-

The Langmuir (equation 6), Freundlich (equation 7), Redlich-Peterson (equation 8), Dubinin-Radushkevich (equation 9), and BET (equation 10) isotherms were fitted to the equilibrium data for the dyes in single dye solutions. The isotherm model fits are displayed in Figure 2a for MO and Figure 2b for RBBR and AR, respectively. The R_{adj}^2 , SD, and adsorption isotherm constants are listed in Table 3. BET isotherm model with the $R_{\text{adj}}^2 > 0.99$ and SD value of 0.073 has the best fit for MO equilibrium data. The MO adsorption on CoAl LDH appears to have a different behavior at lower dye concentration ranges compared to higher concentrations, as observed in Figure 2a. Within the equilibrium MO concentration below 0.08 mmol/L, Langmuir isotherm model describes MO adsorption on the LDH with an R_{adj}^2 of 0.996 and SD value of 0.029 and Freundlich isotherm model has a better fit at higher equilibrium concentration range with an R_{adj}^2 of 0.981 and SD value of 0.073. The MO adsorption behavior on CoAl LDH obtained in this study is similar to the MO adsorption on CoFe LDH studied by Ling et al. (2016), where the authors showed that the Langmuir isotherm

for MO, which was similarly reported by Darmograi et al. (2015) for MO adsorption on MgAl LDH.

MO, RBBR, and AR possess two, four, and three benzene rings, respectively, which can contribute to hydrophobic and π - π interactions between the adsorbed molecules (Ferreira et al., 2017). When two dye molecules approach each other, they require a face-to-face arrangement to increase the chances of π - π interactions. For RBBR and AR, π - π and hydrophobic interactions are likely to be hindered by the steric hindrance caused by the extra sulfonate groups in both the RBBR and AR structures. However, for MO molecules, no additional charged groups are present, which likely favors interactions between the adsorbed and free dye molecules in the solution.

model fit was better at lower equilibrium MO concentrations, whereas the Freundlich model had the best fit at higher concentrations. Therefore, at lower MO equilibrium concentrations, the coverage is a monolayer, whereas at higher concentrations, multilayer adsorption is possible. Dubinin-Radushkevich model describes the RBBR and AR adsorption the best with $R_{\text{adj}}^2 > 0.99$ and $R_{\text{adj}}^2 > 0.98$, respectively and SD value of 0.008. Redlich-Peterson also has a good fit to the RBBR adsorption data with a slightly lower R_{adj}^2 value of 0.984 and higher SD of 0.010 compared to Dubinin-Radushkevich model fit. The adsorption capacity (Q_{dr}) was larger for RBBR (0.265 mmol/g) than for AR (0.199 mmol/g). The magnitude of E obtained from the K_{dr} value using the Dubinin-Radushkevich isotherm model provides information on whether the adsorption process is physical or chemical. For RBBR and AR adsorption on CoAl LDH, E values calculated as 11.18 and 12.91 kJ/mol, respectively are within 8-16 kJ/mol, indicating a chemisorption confirming ligand exchange (Helfferich, 1964).

Comparison of dye adsorption kinetics in single and binary dye solutions of MO and RBBR

As shown in Figure 6a-b, MO adsorption on CoAl reached adsorption equilibrium in less than 250 min for 0.015 mmol/L, 430 min for 0.031 mmol/L, 1630 min for 0.153 mmol/L, and 0.306 mmol/L for the initial dye concentrations. For RBBR (Figure 6c-d), at 430 min, equilibrium was reached for the initial dye concentration of 0.016 mmol/L, 1370 min for 0.032 mmol/L, and 1630 min for 0.160 and 0.319 mmol/L, respectively. When the kinetic data were compared to those obtained in single dye solutions, MO adsorption on CoAl LDH became slower in the binary solution at all initial dye concentrations, whereas the equilibrium time did not change considerably for RBBR.

In the binary solution, the Elovich model described the kinetic data better than the pseudo-second-order model for both MO and RBBR dyes at all initial concentrations (Figure 6). Pseudo-second-order and Elovich model coefficients and constants together with R_{adj}^2 and SD values are presented in Table 4. For MO, both the rate constant (k_2) and the initial adsorption rate (α) decreased in binary solutions compared to the values obtained in single-dye solutions. In contrast, for RBBR adsorption in the binary solution, α increased compared with the values obtained in a single dye solution at all initial dye concentrations.

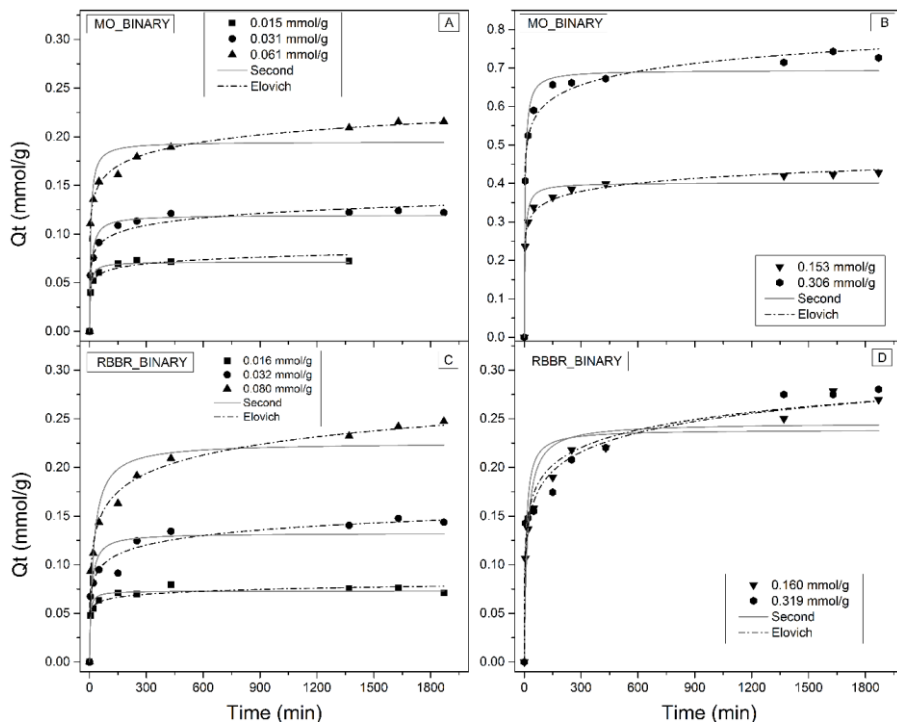


Fig. 6 Pseudo second order kinetics model of MO and RBBR a) MO (Co:0.015-0.061 mmol/L), b) MO (Co:0.153-0.306 mmol/L), c) RBBR (Co:0.016-0.080 mg/L), d) RBBR (Co:0.160-0.319 mmol/L), adsorption on CoAl LDH in single and binary solutions.

Table 4 Kinetics sorption models and related coefficients for binary dye solutions

BINARY	Second order				Elovich					
	C_0 mmol/L	$Q_{e(exp)}$ mmol/g	R_2	SD	K_2 g/min.mmol	$Q_{e(the)}$ mmol/g	R_2	SD	α mmol/g.min	β g/mmol
MO										
0.015	0.071	0.98	0.004	2.841	0.071	0.97	0.004	1.570	161.8	
0.031	0.122	0.96	0.007	0.976	0.119	0.98	0.006	0.667	89.82	
0.061	0.228	0.91	0.020	0.857	0.195	0.10	0.004	1.753	56.43	
0.153	0.448	0.97	0.024	0.533	0.402	0.99	0.011	24.66	32.67	
0.306	0.731	0.97	0.037	0.318	0.694	0.99	0.024	63.28	19.55	
RBBR										
0.016	0.076	0.96	0.005	3.908	0.073	0.96	0.004	73.53	221.0	
0.032	0.145	0.86	0.017	0.741	0.132	0.97	0.008	0.245	71.19	
0.080	0.257	0.89	0.026	0.217	0.225	0.99	0.007	0.114	36.83	
0.160	0.287	0.89	0.029	0.255	0.246	0.99	0.008	0.182	34.99	
0.319	0.280	0.76	0.041	0.477	0.239	0.96	0.018	0.394	38.15	

Comparison of dye adsorption in single and binary dye solutions of MO and RBBR

A comparison of the adsorption capacities of CoAl LDH in single and binary dye solutions for MO and RBBR is

displayed in Figure 7a and 7c, respectively. Figure 7a clearly demonstrates that the adsorption affinity for MO was reduced at all equilibrium dye concentrations when MO and RBBR were present together in the solution matrix.

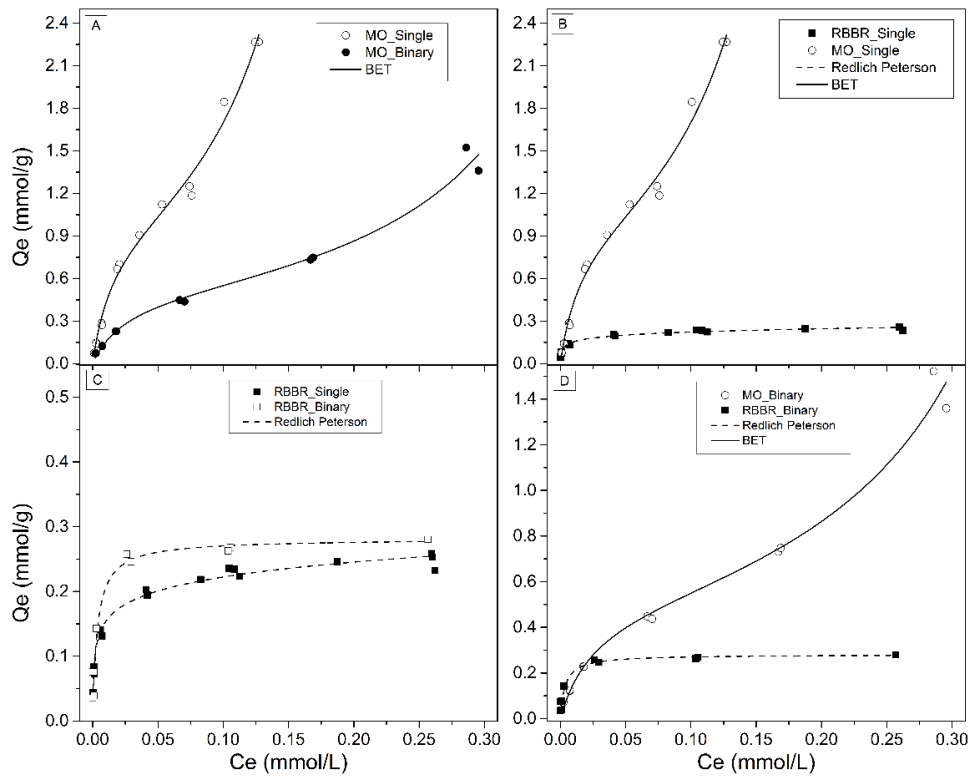


Fig.7 Adsorption isotherm of a) MO in single and binary solutions, b) MO and RBBR in single solution, c) RBBR in single and binary solutions, d) MO and RBBR in binary solution

The highest MO adsorption decreased by ~33% from 2.267 mmol/g in the single-dye solution to 1.521 mmol/g in the binary solution. Surprisingly, the mass of RBBR adsorbed did not change at very low equilibrium dye concentrations up to 0.0025 mmol/L but increased at higher concentrations (Figure 7c). The largest amount of RBBR adsorbed increased by ~4%, from 0.258 mmol/g in the single dye to 0.268 mmol/g in the binary solution.

At equilibrium dye concentrations up to 0.0025 mmol/L, the MO and RBBR molecules may not be influenced by each other because of the presence of excess vacant adsorption sites. At larger surface coverages, cooperative adsorption on solid surfaces is dominated by interactions between adsorbates on the LDH surface. In addition, interactions between the adsorbate adsorbed on the LDH and the adsorbate approaching the neighboring active sites contribute to cooperative adsorption (Liu, 2015). Allen et al., (1988) reported that the reduced mass of dye adsorbed on peat in multisolute matrices is possibly due to three main factors: 1) interactions between the dye molecules in the solution, 2) change in the adsorbent surface charge after the dye adsorption and 3) different dyes competing for the available adsorption sites. In this study, at equilibrium dye concentrations above 0.0025 mmol/L, two possible mechanisms were suggested. First, as MO and RBBR adsorption takes place, negatively charged MO molecules cannot approach the sites occupied by RBBR because of the free negatively charged functional groups available on RBBR molecules, which may explain why the MO mass adsorbed is clearly reduced. Second, the MO molecules adsorbed on CoAl LDH might have preferential intermolecular interactions with the RBBR molecules at higher equilibrium dye concentrations. Hence, the increased RBBR mass

adsorbed in the binary solution can be attributed to the interactions between the MO and RBBR molecules on the LDH surface.

In a single dye solution, at all equilibrium dye concentrations, the amount of MO adsorbed onto the CoAl LDH was higher than the RBBR amount (Figure 7b). However, in the binary solution, the molar mass of RBBR adsorbed was higher than the MO mass adsorbed at equilibrium dye concentrations up to 0.026 mmol/L (Figure 7d). At equilibrium dye concentrations above 0.026 mmol/L, the adsorbed MO molar mass became larger than that of RBBR. Similarly, Chiou and Chuang (2006) showed that chitosan beads had a higher adsorption capacity for RB15 at lower metanil yellow (MY) concentrations, whereas the capacity was higher for metanil yellow at higher MY concentrations in binary solutions. In this study, up to 0.026 mmol/L, surface adsorption due to electrostatic interactions could play a more important role than ligand exchange. RBBR molecules are preferentially adsorbed compared to MO molecules because of their higher electronegativity. At higher concentrations, the hydrophobic properties of MO may enhance adsorption via hydrophobic interactions.

The adsorption isotherm models were fitted to the data obtained in the binary solution, and the R_{adj}^2 and SD values (Table 3) showed that the Langmuir and Redlich-Peterson models best described the RBBR adsorption, while the BET isotherm had the best fit for MO adsorption in binary systems. Maximum adsorption capacity (Q_m) obtained with Langmuir isotherm for RBBR increased from 0.238 mmol/g in single dye solution to 280 mm/g in binary solution while the Redlich constant, a_{RP} decreased

from 789 (mmol/L)^g in single dye solution to 284.5 (mmol/L)^g in binary solutions (Table 3). The changes in the isotherm model constants of both Q_m and a_{RP} indicate that the RBBR adsorption capacity of CoAl LDH increased when MO and RBBR were present together in the solution. The BET constant K_S decreased from 4.728 L/mmol in the single solution to 2.253 L/mmol in the binary solution, while the K_L constant from 68.37 to 40.59 L/mmol. Similar to the behavior of MO in a single dye solution, monolayer adsorption occurred at lower equilibrium concentrations, and multilayer adsorption occurred at higher concentrations (Figure 7a).

Conclusion

The adsorption of MO, RBBR, and AR on CoAl LDH was studied in a single-dye solution, and the mechanisms involved were elucidated. CoAl LDH showed the highest adsorption capacity for MO followed by RBBR and AR. Surface adsorption and electrostatic interactions were considered to play a role in the adsorption of all three dyes, whereas intercalation did not contribute to the adsorption. When tested in a binary dye solution, the adsorption capacity of the CoAl LDH changed considerably. In the solution where MO and RBBR were present together, the mass of MO adsorbed was noticeably reduced at all equilibrium dye concentrations, while the RBBR adsorption increased at equilibrium dye concentrations above 0.0025 mmol/g owing to the cooperative interactions. CoAl LDH had a higher adsorption capacity for MO than RBBR at all equilibrium dye concentrations in single-dye solutions. However, in the binary solution, CoAl LDH showed preferential adsorption for RBBR up to 0.026 mmol/L, while above 0.026 mmol/L, the LDH showed preferential adsorption for MO. The results demonstrated that the dye adsorption capacity of an LDH is highly dependent on the number, characteristics, and equilibrium concentrations of dyes present in a solution, and it cannot be predicted based only on studies conducted in single-dye solutions.

Acknowledgements

The authors thank Abdullahi Isah for helping to conduct some of the characterization analysis of the LDH, Dr. Otar Akanyeti and Dr. Allison Zwarycz for proof reading. This research did not receive any specific grant from funding agencies in the public, commercial, or not-for-profit sectors.

References

- Abdellaoui, K., Pavlovic, I., Bouhent, M., Benhamou, A., Barriga, C. (2017). A comparative study of the amaranth azo dye adsorption/desorption from aqueous solutions by layered double hydroxides. *Applied Clay Science*, 143(Supplement C), 142–150. doi.org/10.1016/j.clay.2017.03.019
- Ada, K., Ergene, A., Tan, S., & Yalçın, E. (2009). Adsorption of Remazol Brilliant Blue R using ZnO fine powder: Equilibrium, kinetic and thermodynamic modeling studies. *Journal of Hazardous Materials*, 165(1–3), 637–644. doi.org/10.1016/j.jhazmat.2008.10.036
- Aguiar, J. E., Bezerra, B. T. C., de Melo Braga, B., da Silva Lima, P. D., Nogueira, R. E. F. Q., de Lucena, S. M. P., da Silva Jr., I. J. (2013). Adsorption of Anionic and Cationic Dyes from Aqueous Solution on Non-Calcined Mg-Al Layered Double Hydroxide: Experimental and Theoretical Study. *Separation Science and Technology*, 48(15), 2307–2316. doi.org/10.1080/01496395.2013.804837
- Allen, S. J., McKay, G., & Khader, K. Y. H. (1988). Multi-component sorption isotherms of basic dyes onto peat. *Environmental Pollution*, 52(1), 39–53. doi.org/10.1016/0269-7491(88)90106-6
- Ay, A. N., Zümreoglu-Karan, B., & Mafra, L. (2009). A Simple Mechanochemical Route to Layered Double Hydroxides: Synthesis of Hydrotalcite-Like Mg-Al-NO₃-LDH by Manual Grinding in a Mortar. *Zeitschrift Für Anorganische Und Allgemeine Chemie*, 635(9–10), 1470–1475. doi.org/10.1002/zaac.200801287
- Bevziuk, K., Chebotarev, A., Snigur, D., Bazal, Y., Fizer, M., & Sidey, V. (2017). Spectrophotometric and theoretical studies of the protonation of Allura Red AC and Ponceau 4R. *Journal of Molecular Structure*, 1144, 216–224. doi.org/10.1016/J.MOLSTRUC.2017.05.001
- Chiou, M.-S., Chuang, G.-S. (2006). Competitive adsorption of dye metanil yellow and RB15 in acid solutions on chemically cross-linked chitosan beads. *Chemosphere*, 62(5), 731–740. doi.org/10.1016/j.chemosphere.2005.04.068
- Choy, J.-H., Kim, Y.-K., Son, Y.-H., Choy, Y. Bin, Oh, J.-M., Jung, H., & Hwang, S.-J. (2008). Nanohybrids of edible dyes intercalated in ZnAl layered double hydroxides. *Journal of Physics and Chemistry of Solids*, 69(5), 1547–1551. doi.org/10.1016/j.jpcc.2007.11.009
- Chung, K. T., Fulk, G. E., & Andrews, A. W. (1981). Mutagenicity testing of some commonly used dyes. *Applied and Environmental Microbiology*, 42(4), 641–648.
- Darmograi, G., Prelot, B., Layrac, G., Tichit, D., Martin-Gassin, G., Salles, F., Zajac, J. (2015). Study of Adsorption and Intercalation of Orange-Type Dyes into Mg–Al Layered Double Hydroxide. *The Journal of Physical Chemistry C*, 119(41), 23388–23397. doi.org/10.1021/acs.jpcc.5b05510
- de Sá, F. P., Cunha, B. N., Nunes, L. M. (2013). Effect of pH on the adsorption of Sunset Yellow FCF food dye into a layered double hydroxide (CaAl-LDH-NO₃). *Chemical Engineering Journal*, 215–216(Supplement C), 122–127. doi.org/10.1016/j.cej.2012.11.024
- Elkhattabi, E. H., Lakraimi, M., Badreddine, M., Legroui, A., Cherkaoui, O., Berraho, M. (2013). Removal of Remazol Blue 19 from wastewater by zinc--aluminium--chloride-layered double hydroxides. *Applied Water Science*, 3(2), 431–438. doi.org/10.1007/s13201-013-0092-3

- Esmaili, S., Ashrafi-Kooshk, M. R., Khaledian, K., Adibi, H., Rouhani, S., Khodarahmi, R. (2016). Degradation products of the artificial azo dye, Allura red, inhibit esterase activity of carbonic anhydrase II: A basic in vitro study on the food safety of the colorant in terms of enzyme inhibition. *Food Chemistry*, 213(Supplement C), 494–504.
doi.org/https://doi.org/10.1016/j.foodchem.2016.06.078
- Ferreira, G. M. D., Ferreira, G. M. D., Hespanhol, M. C., de Paula Rezende, J., dos Santos Pires, A. C., Gurgel, L. V. A., da Silva, L. H. M. (2017). Adsorption of red azo dyes on multi-walled carbon nanotubes and activated carbon: A thermodynamic study. *Colloids and Surfaces A: Physicochemical and Engineering Aspects*, 529, 531–540.
doi.org/10.1016/j.colsurfa.2017.06.021
- Forgacs, E., Cserháti, T., Oros, G. (2004). Removal of synthetic dyes from wastewaters: a review. *Environment International*, 30(7), 953–971.
doi.org/10.1016/j.envint.2004.02.001
- Geethakarthis, A. Phanikumar, B. R. (2011). Industrial sludge based adsorbents/ industrial by-products in the removal of reactive dyes – A review. *International Journal of Water Resources and Environmental Engineering*, 3(1), 1–9.
- Gidado, S. M., Akanyeti, İ. (2020). Comparison of Remazol Brilliant Blue Reactive Adsorption on Pristine and Calcined ZnAl, MgAl, ZnMgAl Layered Double Hydroxides. *Water, Air, & Soil Pollution*, 231(4), 146.
doi.org/10.1007/s11270-020-04522-0
- Goh, K.-H., Lim, T.-T., Dong, Z. (2008). Application of layered double hydroxides for removal of oxyanions: A review. *Water Research*, 42(6–7), 1343–1368.
doi.org/10.1016/j.watres.2007.10.043
- Golka, K., Kopps, S., Myslak, Z. W. (2004). Carcinogenicity of azo colorants: influence of solubility and bioavailability. *Toxicology Letters*, 151(1), 203–210.
doi.org/10.1016/j.toxlet.2003.11.016
- Guo, Y., Zhu, Z., Qiu, Y., Zhao, J. (2013). Enhanced adsorption of acid brown 14 dye on calcined Mg/Fe layered double hydroxide with memory effect. *Chemical Engineering Journal*, 219(Supplement C), 69–77.
doi.org/10.1016/j.cej.2012.12.084
- Hassani, K. El, Beakou, B. H., Kalnina, D., Oukani, E., Anouar, A. (2017). Effect of morphological properties of layered double hydroxides on adsorption of azo dye Methyl Orange: A comparative study. *Applied Clay Science*, 140(Supplement C), 124–131.
doi.org/10.1016/j.clay.2017.02.010
- Helfferich, F. (1964). *Ion exchange*. New York: McGraw Hill.
- Huang, P., Liu, J., Wei, F., Zhu, Y., Wang, X., Cao, C., Song, W. (2017). Size-selective adsorption of anionic dyes induced by the layer space in layered double hydroxide hollow microspheres. *Mater. Chem. Front.*, 1(8), 1550–1555.
doi.org/10.1039/C7QM00079K
- Kumar, P. S., Joshiba, G. J., Femina, C. C., Varshini, P., Priyadarshini, S., Karthick, M. A., Jothirani, R. (2019). A critical review on recent developments in the low-cost adsorption of dyes from wastewater. *Desalin. Water Treat*, 172, 395–416.
- Lei, X., Jin, M., Williams, G. R. (2014). Layered double hydroxides in the remediation and prevention of water pollution. *Energy and Environment Focus*, 3(1), 4–22.
- Lima, É. C., Adebayo, M. A., & Machado, F. M. (2015). Kinetic and Equilibrium Models of Adsorption. In C. P. Bergmann F. M. Machado (Eds.), *Carbon Nanomaterials as Adsorbents for Environmental and Biological Applications* (pp. 33–69). Cham: Springer International Publishing.
doi.org/10.1007/978-3-319-18875-1_3
- Ling, F., Fang, L., Lu, Y., Gao, J., Wu, F., Zhou, M., Hu, B. (2016). A novel CoFe layered double hydroxides adsorbent: High adsorption amount for methyl orange dye and fast removal of Cr(VI). *Microporous and Mesoporous Materials*, 234, 230–238.
doi.org/10.1016/j.micromeso.2016.07.015
- Liu, S. (2015). Cooperative adsorption on solid surfaces. *Journal of Colloid and Interface Science*, 450(Supplement C), 224–238.
doi.org/10.1016/j.jcis.2015.03.013
- Lu, Y., Jiang, B., Fang, L., Ling, F., Gao, J., Wu, F., Zhang, X. (2016). High performance NiFe layered double hydroxide for methyl orange dye and Cr(VI) adsorption. *Chemosphere*, 152(Supplement C), 415–422.
doi.org/10.1016/j.chemosphere.2016.03.015
- McIntok, I. S. (1967). The Elovich Equation in Chemisorption Kinetics. *Nature*, 216, 1204.
doi.org/10.1038/2161204a0
- Momenzadeh, H., Tehrani-Bagha, A. R., Khosravi, A., Gharanjig, K., Holmberg, K. (2011). Reactive dye removal from wastewater using a chitosan nanodispersion. *Desalination*, 271(1–3), 225–230.
doi.org/10.1016/J.DESAL.2010.12.036
- Monash, P., Pugazhenthii, G. (2014). Utilization of calcined Ni-Al layered double hydroxide (LDH) as an Adsorbent for removal of methyl orange dye from aqueous solution. *Environmental Progress & Sustainable Energy*, 33(1), 154–159.
doi.org/10.1002/ep.11771
- Ni, Z. M., Xia, S. J., Wang, L. G., Xing, F. F., Pan, G. X. (2007). Treatment of methyl orange by calcined layered double hydroxides in aqueous solution: Adsorption property and kinetic studies. *Journal of Colloid and Interface Science*, 316(2), 284–291.
doi.org/10.1016/j.jcis.2007.07.045
- O’Hern, Sean C., Michael S. H. Boutilier, Juan-Carlos Idrobo, Yi Song, Jing Kong, Tahar Laoui, Muataz Atieh, and R. K. (2014). Selective Ionic Transport through Tunable Subnanometer Pores in Single-Layer Graphene Membranes. *Nano Lett.*, 14(3), 1234–1241.
- Pereira, L., Alves, M. (2012). Dyes---Environmental Impact and Remediation. In A. Malik & E. Grohmann (Eds.), *Environmental Protection Strategies for Sustainable Development* (pp. 111–162). Dordrecht: Springer Netherlands.
doi.org/10.1007/978-94-007-1591-2_4
- Sajid, M., Basheer, C. (2016). Layered double hydroxides: Emerging sorbent materials for analytical

- extractions. *TrAC Trends in Analytical Chemistry*, 75(Supplement C), 174–182.
doi.org/10.1016/j.trac.2015.06.010
- Saqib, M., Muneer, M. (2002). Semiconductor mediated photocatalysed degradation of an anthraquinone dye, Remazol Brilliant Blue R under sunlight and artificial light source. *Dyes and Pigments*, 53(3), 237–249.
doi.org/10.1016/S0143-7208(02)00024-4
- Silva, T. L., Ronix, A., Pezoti, O., Souza, L. S., Leandro, P. K. T., Bedin, K. C., ... Almeida, V. C. (2016). Mesoporous activated carbon from industrial laundry sewage sludge: Adsorption studies of reactive dye Remazol Brilliant Blue R. *Chemical Engineering Journal*, 303(Supplement C), 467–476.
doi.org/10.1016/j.cej.2016.06.009
- Slama, H. Ben, Chenari Bouket, A., Pourhassan, Z., Alenezi, F. N., Silini, A., Cherif-Silini, H., ... Belbahri, L. (2021). Diversity of Synthetic Dyes from Textile Industries, Discharge Impacts and Treatment Methods. *Applied Sciences*, 11(14).
doi.org/10.3390/app11146255
- Sohrabi, N., Hemmasi, M., Rasouli, N. (2023). Optimization of Adsorption Process Parameters of Allura Red Removal Using Nanodiopside/Zn-Fe Layered Double Hydroxide Composite by Response Surface Methodology: A Kinetic, Thermodynamic, and Equilibrium Approach. *Physical Chemistry Research*, 11(1), 63–78.
doi.org/10.22036/pcr.2022.321821.2009
- Turabik, M., Gozmen, B. (2013). Removal of Basic Textile Dyes in Single and Multi-Dye Solutions by Adsorption: Statistical Optimization and Equilibrium Isotherm Studies. *CLEAN – Soil, Air, Water*, 41(11), 1080–1092.
doi.org/10.1002/clen.201200220
- Wang, Y., Reardon, E. J. (2001). Activation and regeneration of a soil sorbent for defluoridation of drinking water. *Applied Geochemistry*, 16(5), 531–539.
doi.org/10.1016/S0883-2927(00)00050-0
- Wong, Y., Yu, J. (1999). Laccase-catalyzed decolorization of synthetic dyes. *Water Research*, 33(16), 3512–3520.
doi.org/10.1016/S0043-1354(99)00066-4
- Yagub, M. T., Sen, T. K., Afroze, S., Ang, H. M. (2014). Dye and its removal from aqueous solution by adsorption: A review. *Advances in Colloid and Interface Science*, 209(Supplement C), 172–184.
doi.org/10.1016/j.cis.2014.04.002
- Yahya, L. A., Ulfen, I., Kurniawan, F., Jurusan, K. (2016). Pemanfaatan Nata de Coco sebagai Media Gel Elektroforesis Pada Zat Warna Remazol : Pengaruh pH, Waktu dan Aplikasi Pemisahan Gelatin. *JURNAL SAINS DAN SENI ITS*, 5(2), 2337–3520.
- Zaghouane-Boudiaf, H., Boutahala, M., Arab, L. (2012a). Removal of methyl orange from aqueous solution by uncalcined and calcined MgNiAl layered double hydroxides (LDHs). *Chemical Engineering Journal*, 187, 142–149.
doi.org/10.1016/J.CEJ.2012.01.112
- Zaghouane-Boudiaf, H., Boutahala, M., Arab, L. (2012b). Removal of methyl orange from aqueous solution by uncalcined and calcined MgNiAl layered double hydroxides (LDHs). *Chemical Engineering Journal*, 187(Supplement C), 142–149.
doi.org/10.1016/j.cej.2012.01.112
- Zhu, Z., Xiang, M., Li, P., Shan, L., Zhang, P. (2020). Surfactant-modified three-dimensional layered double hydroxide for the removal of methyl orange and rhodamine B: Extended investigations in binary dye systems. *Journal of Solid State Chemistry*, 288, 121448.
doi.org/10.1016/j.jssc.2020.121448
- Zubair, M., Jarrah, N., Manzar, M. S., Al-Harathi, M., Daud, M., Mu'azu, N. D., Haladu, S. A. (2017). Adsorption of eriochrome black T from aqueous phase on MgAl-, CoAl- and NiFe- calcined layered double hydroxides: Kinetic, equilibrium and thermodynamic studies. *Journal of Molecular Liquids*, 230(Supplement C), 344–352.
doi.org/10.1016/j.molliq.2017.01.031